Dynamics of spray – swirl – acoustics interactions

Kumara Gurubaran. R., and Sujith R. I.*

Department of Aerospace Engineering, IIT Madras, Chennai – 600036, India.

Received on 31st January 2010, Revised submission on 20th July 2010; Accepted on 13th September 2010

ABSTRACT

Combustors with fuel-spray atomizers are particularly susceptible to pressure or velocity oscillations resulting from the occurrence of thermoacoustic oscillations. Experimental investigations of distilled water spray – swirl – acoustic interactions are presented. The presence of a swirl flow field alters the behavior of water spray drastically. Investigations showed complex behavior of water sprays in an acoustic cycle. In the presence of acoustic oscillations the phase averaged droplet diameter variation with in an acoustic cycle is more at the axial locations compared with off axis locations. The phase averaged axial velocity variation of the droplets is high compared to that of phase averaged radial and tangential velocities with in an acoustic cycle. Periodic clustering of droplets in the spray field is observed in the presence of acoustic field. A maximum particle count of 14 times the minimum count in a phase angle bin is observed within an acoustic cycle for the acoustic pressure amplitude of 3000 Pa. The droplet diameter distribution in the spray field is affected in the presence of acoustic oscillations.

1. INTRODUCTION

Despite the many advances in combustor design, the challenge to ingenuity in design is now greater than ever before. This is because of the increased interest in the environment, ozone depletion, energy conversion efficiency etc. by scientists and the general public. In the primary zones of the combustor featuring spray fuel injection, the pattern of burning is highly complex. The emission of pollutants, including NOx are influenced by the physical process of atomization, evaporation, and fuel/air mixing associated with flow in addition to the mean velocity that provides information on the residence time distribution in the entire flow field [1]. The combustor must burn the fuel completely with the smallest possible pressure drop to produce gases of uniform temperature and maintain stable combustion over a wide range of operating conditions. This is accomplished by imparting swirl to the flow field [2]. Swirl flows are generally associated with recirculation regions which stabilize the flame and enhance mixing, thereby improving the NOx reduction [3].

Prof. Yannis Hardalupas served as the sole independent editor for this paper

*Corresponding author; email: sujith@iitm.ac.in

Spray combustion is an inherently unstable mechanism because of the unsteadiness involved in the evolution of sprays. Further, spray combustion cannot be truly designated as premixed or as diffusion combustion process as in the case of gaseous combustion. In gas turbine combustors, the fuel is injected into a swirling flow field. Swirling flows are highly three dimensional and it is quite complex to obtain enough details experimentally to fully comprehend the mechanisms involved. The atomization process is highly unsteady, involving several interacting mechanisms and is quite complex.

Rizkalla and Lefebvre [4] investigated in detail the effects of both air and liquid properties on airblast atomization quality. Rizkalla and Lefebvre drew certain general conclusions concerning the main factors governing the mean drop size. For liquids of low viscosity, the key factors are surface tension, air velocity and air density. They concluded that liquid viscosity has an effect which is quite separate and independent from that of air velocity.

Aerodynamic characteristics of swirling spray flames in a pressure jet atomizer was investigated by Presser et al. [5]. They reported that the introduction of swirl to the combustion air modified the droplet and air velocity field and the spatial distribution of droplet size and number density. Presser et al. [6] examined the droplet transport in a swirl- stabilized kerosene spray using laser velocimetry and phase Doppler interferometry at nonburning and burning conditions. They reported from the time series of velocity data at different spatial locations that the spray showed some intermittency and clustering of droplets. Size classified interpretation of droplet velocity data in the swirling flames [7] showed that droplet drag were sufficiently strong on small sized droplets. The effect of combustion on droplet transport was examined by Gupta et al. [8] by comparing the burning and nonburning spray under similar flow conditions. Combustion enhanced the droplet vaporization that resulted in reduced number density and larger mean droplet mean diameter and velocities when compared to the nonburning spray. Jeng et al. [9] investigated the non-reacting spray characteristics issued from a counter-rotating swirler. They reported that the smaller droplets tend to follow the vertical breakdown flow structure recirculating back towards the nozzle inside the hollow-cone spray and the larger droplets retained their trajectory because of increased momentum.

In the past, investigations were performed to understand the behavior of evaporative and non-evaporative sprays in the presence of acoustic oscillations [10-13]. To summarize, the diameter distribution and velocity of droplets in the spray field varies spatially. The investigations of various researchers showed that the droplets in the spray are entrained in the vortical structures developed due to acoustic forcing. Further, the resonant acoustic oscillations in the combustors increased the evaporation rates compared to the steady state evaporation rates. There was a droplet number density wave in the presence of the air velocity fluctuations propagating with convective velocity [14]. The effects of acoustic oscillations on the spray were stronger when the spray was located at an acoustic velocity anti-node and were minimal when located at an acoustic velocity node.

Anderson et al. [15] measured the spray/ acoustic coupling in gas turbine fuel injectors using the fluorescence of additives and aromatic constituents in the fuel. They identified strong acoustic coupling between the pulsed air flow and the fuel spray mass flow at the frequency range from 350 to 650 Hz for the injectors tested.

Brena de la Rosa et al. [16] studied the effect of swirl on the structure and on velocity and turbulence fields of a liquid spray. They measured the dynamic properties of air and the spray for three types of vane swirlers of swirl number 0.26, 0.40 and 1.23 using PDPA and two component LDV. They concluded that the spatial distribution of sizes and velocities, the particle number density and the liquid volume flux of the spray are strongly influenced by the dynamics imposed by the swirling field. Droplets experienced flow reversal under the effect of a high swirl number. High swirl number produced more homogeneous distribution of mean drop sizes due to vigorous mixing induced by higher turbulence intensity. The effect of combustion instability on the structure of recirculation zones in confined swirl flames was investigated by Dawson et al. [14]. They reported that the significant deformations to the flow structure occur in axial velocity field than the tangential velocity field due to the unsteady pressure amplitudes. The small amplitudes of unsteady pressure introduced comparatively large axial velocity amplitudes in the recirculation zone. They reported that the flame dynamics are not a direct response to small amplitude pressure oscillations but rather a direct response to changes in the local flow velocity that was determined by the phase velocity at the burner exit.

The behavior of spray downstream of an aeroengine injector with acoustic excitation was investigated by Gajan et al. [17]. They created periodic fluctuations in the pressure and velocity by modifying the downstream nozzle area periodically. They stated that the spray exhibited a droplet number density wave formed mainly with smaller droplet sizes.

Arunraj et al. [18] investigated the effect of acoustic oscillations on swirl flow from a vane type swirler in a confined geometry. His results showed that the fluctuations in axial velocities in the recirculation zone are much higher than the acoustic velocity and no significant change in the tangential velocity. He concluded that the acoustic oscillations helped in delocalizing the vorticity patches, thus enhancing mixing.

Most gas turbine injectors employ swirl configurations that produce central toroidal recirculation zones (CTRZ) to provide the dominant flame stabilization mechanism. It is reported that fluctuations in axial velocities in the recirculation zone are higher than that of acoustic velocity corresponding to the standing wave and the effect on the tangential velocity component is negligible. However, few studies deal with the fundamental aspects of swirl – spray – acoustics interactions.

2. EXPERIMENTAL SETUP

The experimental setup employed in the present study is shown in Fig. 1. This includes a pressurized air supply system, a liquid supply system, an injector assembly and, a duct attached with electromechanical acoustic drivers for generating standing waves. The length of the aluminum duct is 1050 mm with square cross section of side 150 $\times$ 150 mm. The top end of the duct is closed and the other end is open to the atmosphere. A photographic view of the swirler and the air-assist atomizer mounted in the frontal

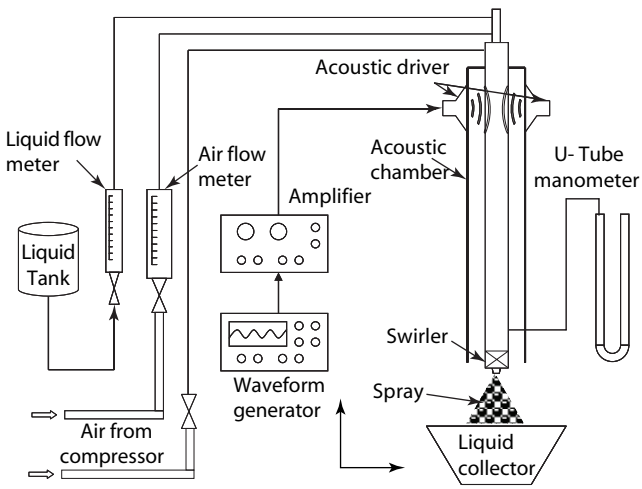

Fig. 1 Schematic of the experimental set-up

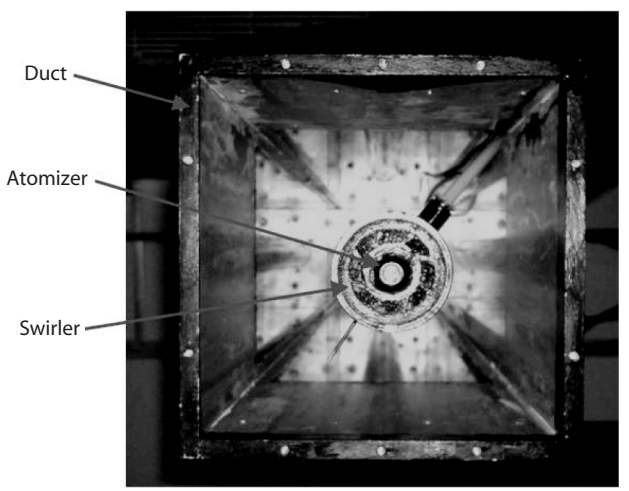

Fig. 2 Photographic view of the swirler and the air-assist atomizer mounted in the frontal adapter.

adapter is shown in the Fig. 2. The nozzle used in the present study is an air-atomizing nozzle, Delevan 30609, that produces a solid cone spray. The nozzle is mounted on a frontal device adapter. The frontal device adaptor houses the swirler and nozzle. Four synchronized electromechanical acoustic drivers fitted to the closed end of the setup were used to excite standing waves of chosen frequency and amplitude (longitudinal modes). Amplitudes in excess of 3000 Pa were attained in the test section. For the acoustic pressure measurement inside the duct and at the closed end of the duct,

pressure transducers (PCB model number 106B50) with a sensitivity of 78.4 mV/kPa and uncertainty of +/− 0.8% are used. The liquid used in the present study is distilled water (from here on, water means distilled water). The flow rate of the liquid and air to the nozzle are controlled using a needle valve and measured using a rotameter of 2 % accuracy. The air flow to the swirler is controlled using a needle valve and the pressure drop across the swirler is measured using a U-tube manometer.

The visualization of the spray field is based on the Mie scattering of droplets in the spray field. A pulsed, frequency doubled, Nd-YAG laser is used for spray visualization experiments. More than 500 instantaneous images were acquired and ensemble averaged.

The droplet size and velocities of the spray field were performed using a three component PDPA system (TSI, USA). The laser used for the present experimental study is an Argon Ion laser (Coherent Innova 70C, USA, make). The multicolor laser beam is split and separated into three pairs of colors; i.e., green (514.5 nm), blue (488 nm) and violet (476.5 nm). In the present study, only two components were measured. One part of each pair of the beam is shifted by 40 MHz from the other. The green and blue pairs of beams go to one fiber optic transceiver probe. The fiber optic transceivers are mounted on a three axis traverse system, whose movement is controlled remotely from a computer. The green pair of beams is aligned in the main flow direction with respect to the receiver optics. The data is phase locked with the acoustic signal generated by the electromechanical acoustic drivers. The PDPA system was set-up to optimal measurement conditions [19, 20]. The transmitting optics focal length is 261 mm, resulting in probe volume of 61 µm. The optical arrangement allowed to measure droplet diameters up to 85 µm. The signal to noise ratio was set at high. Valid droplet size measurement are obtained after passing through the droplet intensity validation based on d^2 law (scattered light intensity being proportional to the square of droplet diameter) and coincidence on all channels of measurement. The size distribution and the mean diameters at each point were based on more than 30,000 valid data measurements with statistical uncertainties of less than 2%. The worst case uncertainty in the velocity measurements with the measured mean velocity is 1.2% [21].

Experimentally measured resonant frequencies of the acoustic chamber are 238, 391 and 540 Hz, i.e, first, second and third harmonic respectively [13]. The measured resonant frequencies has uncertainty of +/- 1 Hz. Figure 3 shows the phase averaged acoustic velocity oscillations (over mean) at the exit of the duct for various acoustic pressure amplitudes at an excitation frequency of 238 Hz. The investigations of swirl – spray – acoustic interactions are performed at duct resonant frequency of 238 Hz and for various acoustic pressure amplitudes are presented in this paper. It was difficult to attain higher acoustic pressure amplitudes (3000 Pa) at resonant frequencies of 391 and 540 Hz with the acoustic drivers used in the present investigations. The investigations at lower acoustic pressure amplitudes (1000 Pa) at 391 and 540 Hz showed similar results as of 238 Hz. The droplet size measurements of water spray were performed at a cross-sectional plane 25 mm downstream from the atomizer exit and at radial locations 0 mm to 30 mm with an interval of 5 mm. The measurements are phase locked with the acoustic pressure measured at the closed end of the acoustic chamber, so that each valid measurement acquired from the spray field under investigation is tagged with the

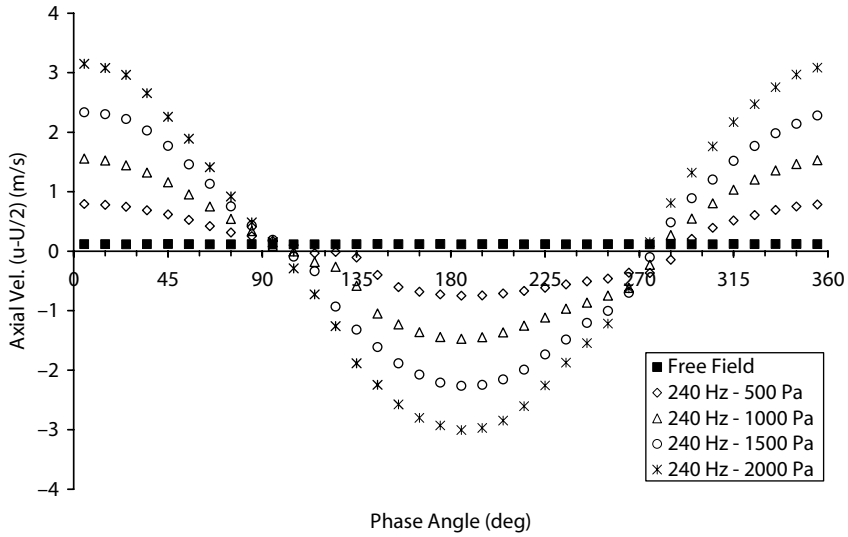

Fig. 3 Phase averaged acoustic velocity oscillations (over mean) at the exit of the duct for various acoustic pressure amplitudes at an excitation frequency of 238 Hz.

respective phase angle of the acoustic cycle. More than 1,00,000 valid droplet size measurements are acquired

3. RESULTS AND DISCUSSION

The axial acoustic velocity field at the open end of the acoustic chamber is characterized first and the details are given in Kumara Gurubaran et al. [13]. The area averaged initial velocity of the liquid jet at the atomizer exit is 2.1 m/s. The area averaged initial velocities of the atomizing air for the three experimental conditions investigated at the atomizer exit are 32.7, 49.1 and 65.5 m/s. This leads to a Weber number (*We*) defined as $\rho_A U_R^2 D/\sigma$ (where ρ_A is the air density, U_R is the relative velocity between the atomizing air and the liquid, D is the diameter of the liquid jet, and σ is the surface tension) of 7.7, 18.2 and 33. With the acoustic pressure expressed A sin ($\omega t + \phi$) the reference phase 0° corresponds to $\phi = 0°$. A pressure drop of 0.03 bar is maintained constant across the swirler for all the experiments. The mean velocity and Re at the swirler inlet are 5.3 m/s and 15300, respectively.

To envisage the swirl – spray – acoustic interactions in flow field an illustration depicting the effect of acoustic velocity oscillations on the swirl flow field is shown in Fig. 4. The jet with high degree of swirl has high swirl momentum and kinetic energy at the exit of the swirler. This momentum and kinetic energy is exhausted gradually downstream by aerodynamic resistance. Swirl flow generates large radial pressure gradients due to centrifugal effects. This causes a sub-atmospheric low pressure region in the central region of the flow, this region is known as the central toroidal recirculation

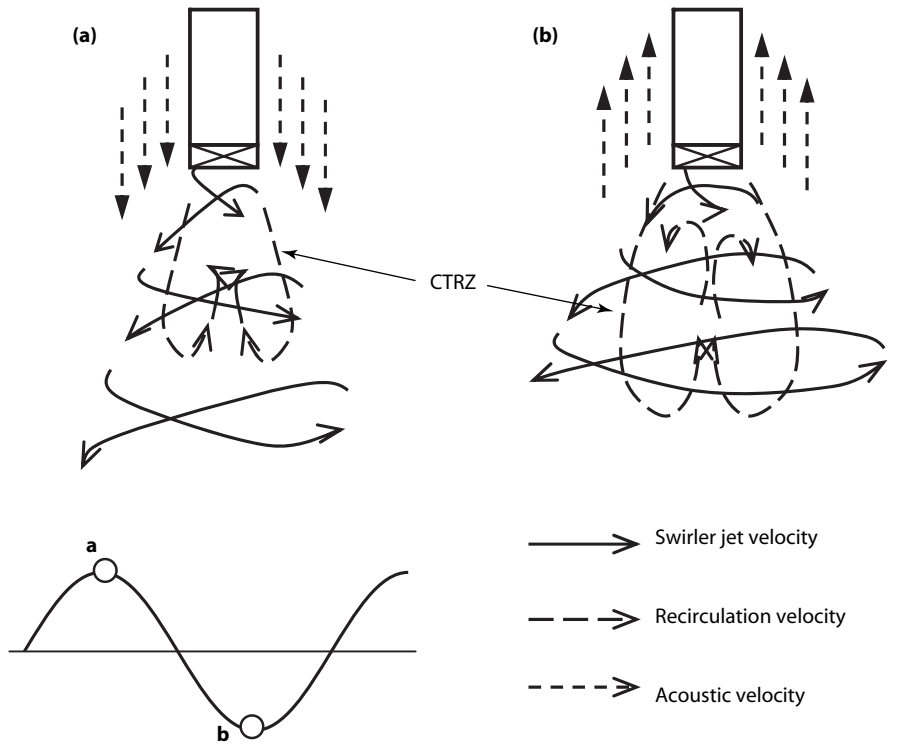

Fig. 4 Illustration showing the effect of acoustic velocity oscillations on the swirler flow field.

zone (CTRZ). In a co-flowing acoustic velocity, the swirler jets exiting from the swirler has an unrestricted flow field. The shear between the swirler jet and the co-flowing acoustic velocity is less. This causes the swirler jet to penetrate further downstream until its momentum is exhausted (Fig. 4a). The recirculation velocity and the size of CTRZ are reduced in co-flowing acoustic velocity. Counter-flowing acoustic velocity restricts the swirl flow by increasing the relative velocity between the swirler jets and the surrounding medium. The relative velocity is high in counter-flowing acoustic velocity. This increase in relative velocity increases the shear that aids in faster dissipation of the swirler jet momentum in the surrounding medium. Hence, the penetration and the velocity of the swirler jet is reduced. The recirculation velocity and the size of CTRZ are increased in counter-flowing acoustic velocity (Fig. 4b). The air-assist atomizer is located in the recirculation zone. The droplets are entrained by the swirl flow field which in turn has response to the acoustic oscillations. This shows the complexity of the problem investigated though in a simplified form of the actual gas turbine combustion model.

3.1 Planar Spray Field Visualization

The instantaneous planar Mie scattering images of the water spray field in the presence and absence of the swirl flow field for different *We* are shown in Fig. 5. The images

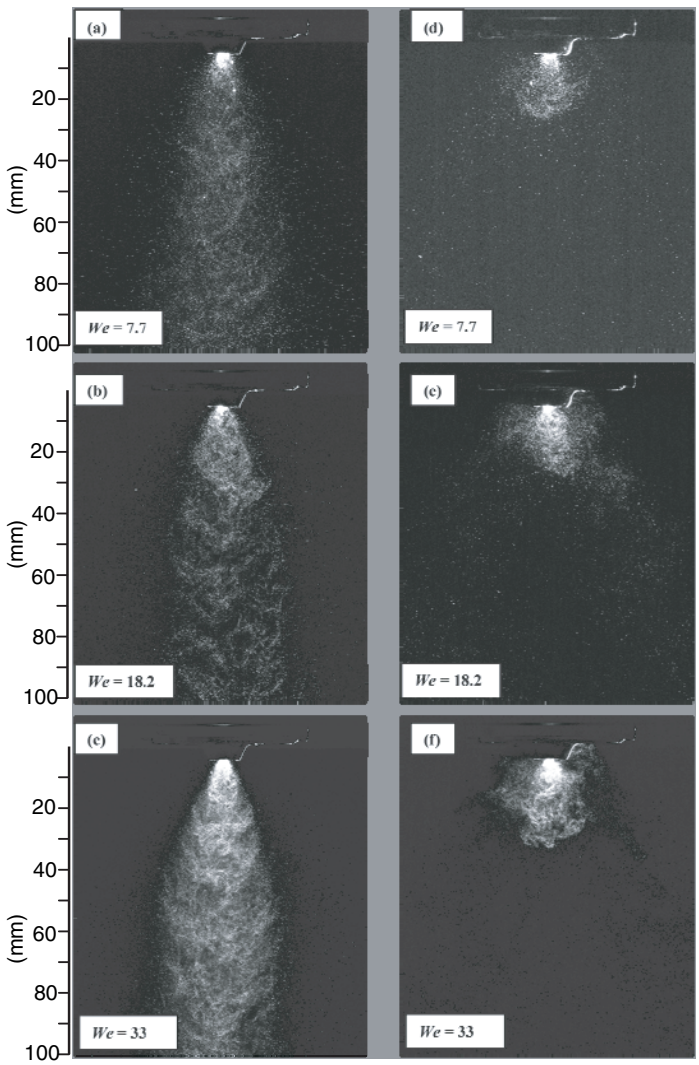

Fig. 5 Instantaneous planar Mie scattering images of the spray field for different *We* in absence of swirl flow field a) *We* = 7.7, b) *We* = 18.2 and c) *We* = 33 and in the presence of swirl flow field d) *We* = 7.7, e) *We* = 18.2 and f) *We* = 33.

presented are brightened for better visualization and understanding. The raw images have a gray scale resolution of 12 bits with intensity scale range of 0 to 4095, and care is taken to ensure that the individual images are not saturated by adjusting the laser power and the camera aperture. The optical parameters of the planar Mie scattering imaging are maintained constant for all the investigations.

The instantaneous image in Fig. 5a for *We* of 7.7 shows that the droplets in the spray field in the absence of swirl flow are more dispersed in planar Mie scattering. The instantaneous image in Fig. 5b for a *We* of 18.2 shows the droplets in the spray field are closer (i.e., a denser spray) compared to *We* of 7.7. Further increase in the *We* causes the droplets to be very closely packed, increasing the droplet number density, as observed in Fig. 5c for a *We* of 33. Increase in the *We* increases the droplet number density of the spray field. The *We* is varied by varying the volume flow rate of the air through the atomizer.

In the presence of swirl flow, the water spray field is altered drastically as it is evident from Fig. 5 d, e & f. In the presence of swirl, the liquid dispersion increases and mixes rapidly with the surrounding continuous medium. The instantaneous image in Fig. 5d for *We* of 7.7 shows that in comparison with Fig. 5a the droplets in the spray field in the presence of swirl flow are more dispersed. The penetration of the spray from the air-assist atomizer is reduced. With the atomizer positioned in the hub of the swirler and both are housed in the frontal adaptor, the solid cone spray is injected into CTRZ formed by the swirl flow. The reverse flow in the recirculation zone opposes the spray jet velocity. Hence, the spray penetration is less and the droplets in the spray field are carried away with the swirling flow of the surrounding continuous (air) phase. The kinetic energy and droplet number density of the spray field is increased with increase in *We*. The *We* is varied by varying the volume flow rate of the air through the atomizer. Increase in air velocity is beneficial to the atomization quality. For liquids of low viscosity, the mean drop size is inversely proportional to the relative velocity between the air and the liquid (water) phases at the nozzle exit [22]. The increase in kinetic energy of the spray causes it to penetrate more into the CTRZ of the swirl flow field. Increase in the *We* to 18.2 has increased the penetration of spray (Fig. 5e). Further increase of *We* to 33 increases the droplet number density and penetration of the spray into the CTRZ of the swirl flow field (Fig. 5f). An examination of instantaneous planar Mie images of the spray field shows that the flow field is highly unsteady in presence of a highly three dimensional swirl flow field having a high degree of swirl (1.03).

Contour plots of ensemble averaged planar Mie scattering images of the spray field for different *We* in the absence and presence of swirl flow field are shown in Fig. 6. The pressure drop across the swirler is 0.03 bar and the mean velocity and *Re* at the swirler inlet are 5.3 m/s and 15300, respectively. The spray droplet number density increases with increase of *We*, both in the presence and in the absence of the swirl flow field. The spray angle decreases with increase in *We*. In the contour plot of *We* 7.7 (Fig. 6a), the spray field width is more compared with that of *We* 18.2 (Fig. 6b). Further increase in the *We* causes the width of the spray field outer boundary to reduce (*We* = 33 in Fig. 6c). Increase in the *W*e increases the momentum and kinetic energy of the droplets in the spray field causing it to penetrate more. Thereby, the width of the spray outer boundary is decreased. In the presence of the swirl flow field, it is observed that the penetration is drastically altered and the spray field is highly dispersed in the surrounding continuous (air) phase. The spray penetration is governed by the relative magnitudes of the kinetic energy of the initial spray from the atomizer and the aerodynamic resistance and the interaction of the surrounding continuous phase. The initial kinetic energy of the spray is usually high. The

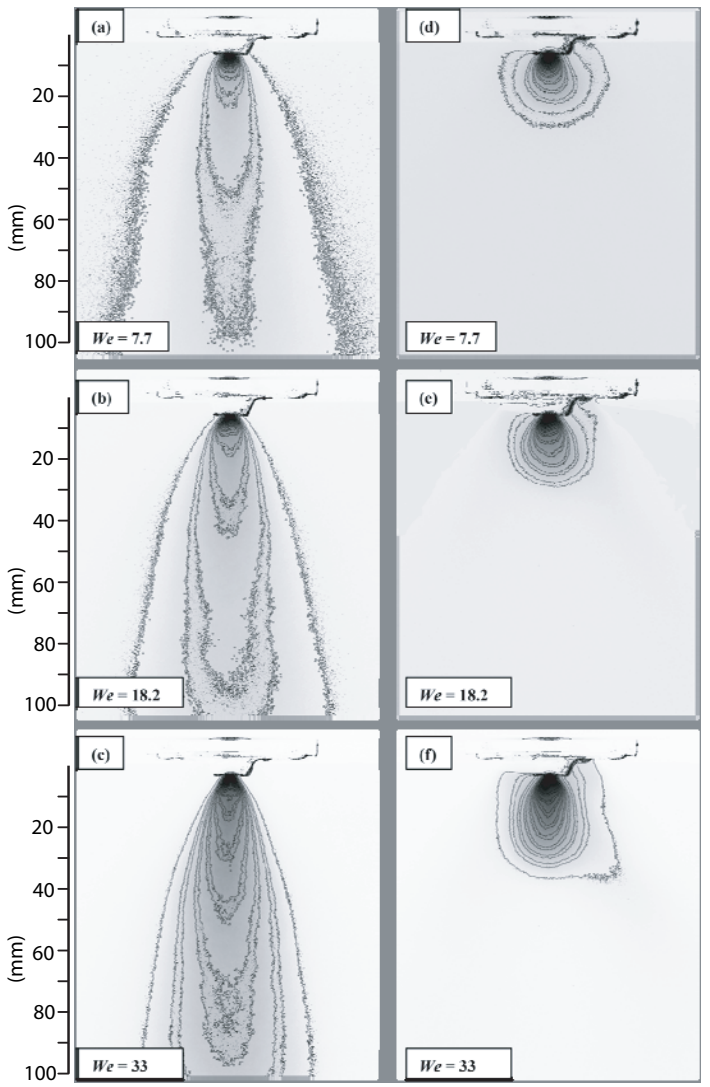

Fig. 6 Contour plots of ensemble averaged planar Mie scattering images of the spray field for different We in absence of swirl flow field a) *We* = 7.7, b) *We* = 18.2 and c) *We* = 33 and in the presence of swirl flow field d) *We* = 7.7, e) *We* = 18.2 and f) *We* = 33

kinetic energy is gradually dissipated by frictional losses to the continuous phase. Finally, when the kinetic energy of the droplets in the spray is exhausted, mainly gravity and the movement of the surrounding continuous phase dictate their subsequent trajectory. This explains the high dispersion.

3.2 Droplet Size and Velocity of Spray in the Swirl Flow Field

Droplet size measurements of the water spray field in the presence of swirl were performed at a cross-sectional plane 25 mm downstream from the atomizer exit and at radial locations 0 mm to 30 mm with an interval of 5 mm. Since the droplet number density in the flow field is less for *We* of 7.7 and 18.2 compared to that of 33 in the presence of swirl flow, *We* of 33 is chosen for the droplet size and velocity measurements of the spray field. At lower droplet number density, it is very difficult to get required number of valid droplet measurements. The spray penetrates the CTRZ up to 25 mm downstream from the atomizer exit for a *We* of 33. Figure 7a shows the radial variation of diameters D_{10} and D_{32}. The maximum mean diameters are between locations 10 mm to 15 mm off axis 25 mm downstream location from the atomizer exit.

Penetration of the spray field is reduced in the presence of swirl flow as explained in Section 3.1 (Fig. 5). In general, bigger size droplets are in the periphery of the solid

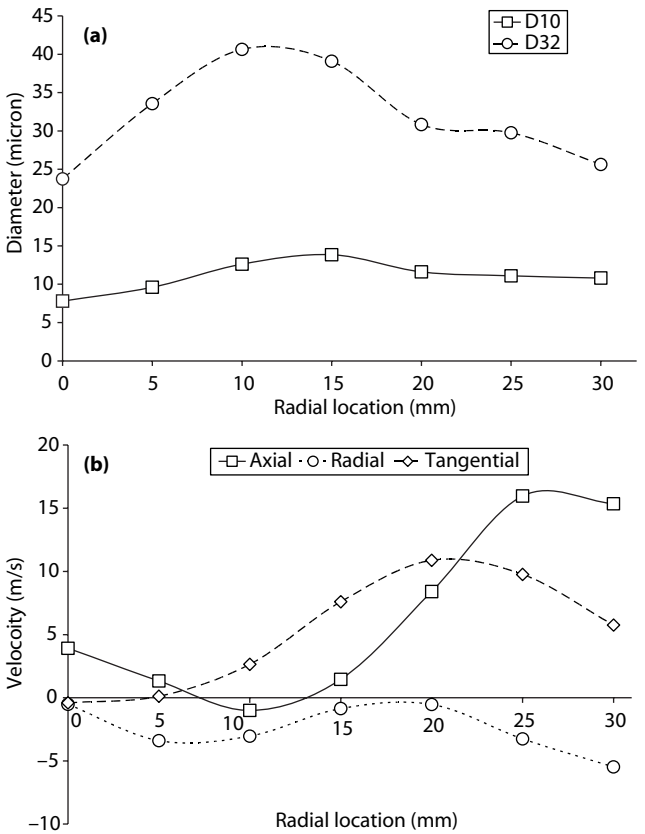

Fig. 7 a) Radial variation of droplet size and b) 3-component velocities of the droplets in the presence of the swirl flow field at 25 mm downstream from the atomizer exit for *We* of 33.

cone spray (in the absence of swirl). The outer periphery of the solid cone spray is around 13 mm in radius from the axis at 25 mm downstream from the atomizer exit, as observed from the planar visualization (in the absence of swirl). The velocity of the continuous medium is in the opposite direction to the spray in the CTRZ region of the swirl flow field [22]. The velocity of continuous medium in the opposite direction to spray in the presence of swirl flow causes the spray droplets to exhaust their kinetic energy, and the droplets are accumulated. These accumulated droplets are entrained by the swirl flow field and carried away along with the flow. The mean diameter of the spray decreases beyond 20 mm in the radial direction. The spray droplets present in these radial locations are entrained by the swirler flow and carried away by it.

The radial profiles of the mean axial, radial and tangential droplet velocities at 25 mm downstream from the atomizer exit are shown in Fig. 7b. Axial velocity of droplets is 4 m/s at the axis of atomizer. Then the axial velocity of the droplets decreases to 1.5 m/s at 10 mm radial location and increases at radial locations away from the axis of atomizer. The decrease in axial velocity of droplets from the axis up to 10 mm radial location and then increases at radial locations away is due to the interaction of the swirl flow with the droplets in the spray field. The width of the recirculation zone at 25 mm downstream from the atomizer exit is from -15 mm to 15 mm in the cross-sectional plane determined from the PIV measurements [23]. The mean velocity of droplets is positive at the axis because the droplets penetrate the CTRZ and have kinetic energy present in them. The radial and tangential velocities of the droplets approach zero at the axis of the spray field. The mean tangential velocity of the droplets is negligible at an axial location 25 mm downstream from the atomizer exit. The mean tangential velocity increases in radial locations away form the atomizer axis up to 20 mm in radius. This shows the presence of a strong swirling flow field. Beyond 20 mm in radial locations, the tangential velocity of droplets decreases and the number density of droplets also decreases.

The spray is drastically altered in the presence of swirl flow as observed from the planar spray field visualization experiments. The droplets in the spray field are thrown apart due to the centrifugal force and the spray penetration is considerably reduced in the presence of the swirl flow. The CTRZ of the swirl flow field affects the mean droplet velocities of the water spray significantly compared with the droplet velocities of the spray in the absence of the swirl flow. The droplet number density also varies from location to location in the presence and absence of the swirl flow field. Therefore, it is not apt to compare the droplet size and velocity measurements of the spray field in the absence and with the presence of swirl flow for the kind of atomizer and swirler arrangement in the frontal device adaptor that is used in the present investigations. However, at some locations an attempt is made to compare the results in the presence and absence of swirl flow.

3.3 Effect of Acoustic Field on Droplet Size

The effect of swirl on spray droplet size in the presence and absence of acoustic field is investigated. The droplet size measurements of water spray were performed at a cross-sectional plane 25 mm downstream from the atomizer exit and at radial locations 0 mm to 30 mm with an interval of 5 mm. The measurements are phase locked with the

acoustic pressure measured at the closed end of the acoustic chamber, so that each valid droplet measurement acquired from the spray field under investigation is tagged with the respective phase angle of the acoustic cycle. More than 1,00,000 valid droplet size measurements are acquired. However, at the outer periphery, the data rate is very low. Hence, valid droplet size measurements of about 40,000 are obtained at the outer periphery. The valid measurements of drop sizes are grouped into 20° phase angle bins. Drop sizes in each phase angle bins (total of 18 phase angle bins) are averaged to obtain the drop size variation of the spray field within an acoustic cycle. The acoustic velocity is co-flowing (outward from the acoustic chamber) to the swirl – spray field between the phase angles 0° to 90° and 270° to 360° (0°). The acoustic velocity is counter-flowing (into the acoustic chamber) to the swirl – spray field between the acoustic phase angles 90° to 270° [24].

The phase averaged droplet diameters D_{10} and D_{32} in the spray are altered within an acoustic cycle in the presence of acoustic field. Figure 8a shows the variation of phase

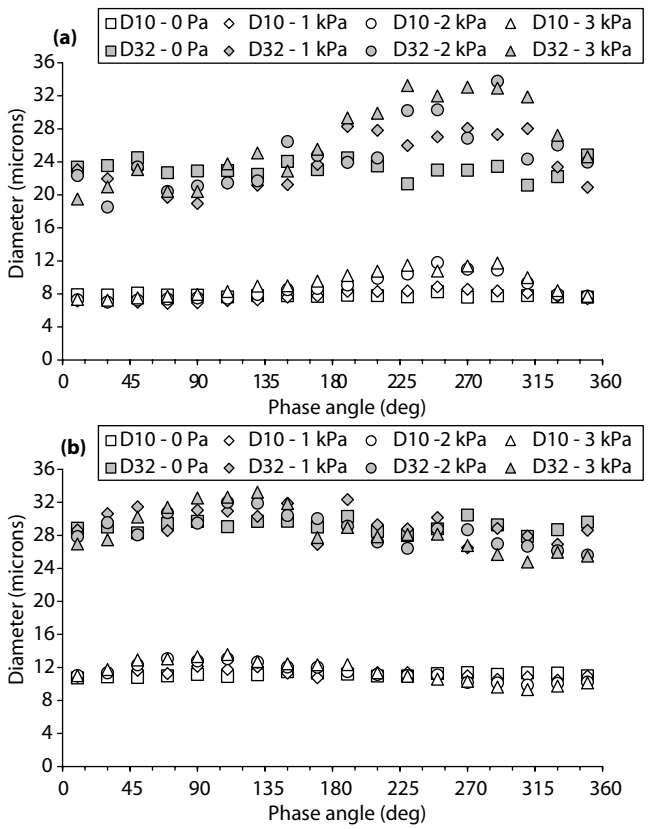

Fig. 8 Phase averaged diameter of droplets at 25 mm downstream from the atomizer exit at a) axis and b) 25mm off axis locations, at 238 Hz and for various pressure amplitudes.

averaged diameters of the spray field at 25 mm downstream along the axis from the atomizer exit at a frequency of 238 Hz for various pressure amplitudes. A variation of 24%, 43% and 52% in D_{10} and 27%, 40% and 54% in D_{32} phase averaged diameters within an acoustic cycle over the mean droplet diameters are observed for acoustic pressure amplitudes of 1000 Pa, 2000 Pa and 3000 Pa, respectively. The variation of phase averaged diameters in an acoustic cycle is high, around ~10% in the case of spray – swirl – acoustics interactions compared to that of the spray field in acoustic excitation in the absence of swirl flow. However, the spray is injected into the recirculation region in the investigation of spray – swirl – acoustic interactions. The relative velocities of the droplets in the spray are increased in the presence of swirl flow compared to that in the absence of swirl flow [13]. The variation in phase averaged droplet diameters D_{10} and D_{32} within an acoustic cycle increases with the increase in the acoustic velocity oscillations in the acoustic chamber. Variation of phase averaged diameter D_{10} is similar to the variation of phase averaged diameter D_{32}. The mean droplet size increase in the presence of acoustic field over the absence of acoustic field between the phase angles of 200° to 330° (Fig. 8a). A decrease in D_{32} is observed between the phase angles of 0° to 90°.

Figure 8b shows the variation of phase averaged diameters of the spray field at 25 mm downstream from the atomizer exit at a location 25 mm off axis, at 238 Hz and for various pressure amplitudes. A variation of 15%, 27% and 37% in D_{10} and 13%, 20% and 28% in D_{32} phase averaged diameters within an acoustic cycle over the mean droplet diameters are observed for acoustic pressure amplitudes of 1000 Pa, 2000 Pa and 3000 Pa, respectively. The variation in phase averaged droplet diameters within an acoustic cycle increases with the increase in the acoustic velocity oscillations in the acoustic chamber. The variation of droplet size within an acoustic cycle is less at 25 mm off axis location compared to the variation in droplet size at the axis. This can be due to the variation in the phase averaged axial velocity of the droplets being high at axial locations compared to that of off axis locations in an acoustic cycle in the presence of acoustic field. This is discussed in the Section 3.4. A similar trend in the variation of phase averaged diameter D_{10} and D_{32} within an acoustic cycle is observed at off axis location. However, the percentage of variation in phase averaged droplet size within an acoustic cycle is more in D_{10} compared to that of D_{32} (Fig. 8b). Phase averaged droplet size increases in the presence of acoustic field over the absence of acoustic field between the phase angles of 30° to 150° (Fig. 8b). Decrease in diameters is observed between the phase angles of 240° to 360°. The trend in variation of phase averaged droplet diameters within an acoustic cycle is different at on-axis and off-axis locations.

The radial variation of phase averaged droplet size in the presence of acoustic oscillations at different phases in an acoustic cycle, for a frequency of 238 Hz and pressure amplitude of 3000 Pa is shown in Fig. 9. The magnitude of variation in mean droplet diameter, D_{10} within an acoustic cycle varies from location to location.

At a phase angle of 10°, the phase averaged droplet diameter D_{10} is minimum at the axis and increases to a maximum at the 10 mm off axis. This phase angle corresponds to the co-flowing acoustic velocity [24]. The velocity in the recirculation region is reduced and the velocity of jets from the swirler vanes are increased in co-flowing acoustic velocity [23]. Due to decrease in recirculation velocity in CTRZ, the spray

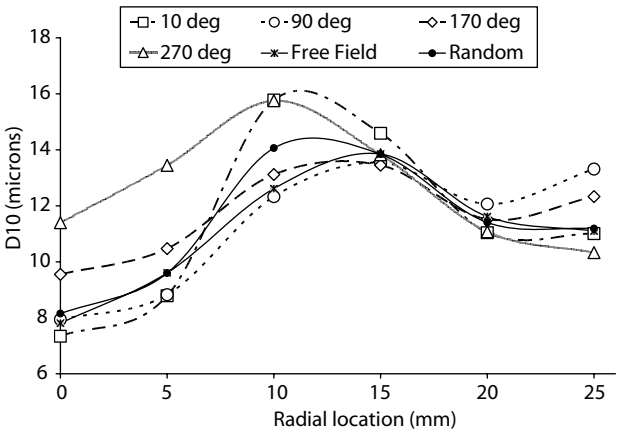

Fig. 9 Radial variation of phase averaged diameter of droplets at 25 mm downstream from the atomizer exit at 238 Hz and for pressure amplitude of 3000 Pa.

penetrates more and the droplet sizes are minimum at the axis of solid cone sprays. At 15 mm and 20 mm off axis, the variation in the phase averaged droplet diameter within in an acoustic cycle is less compared to other radial locations.

The phase averaged droplet diameter variations in the radial locations show a very complex behavior in the presence of acoustic field. Spray in a strong swirl flow field is itself highly complex and highly three-dimensional. Non-uniformities in the fuel distribution in gas turbine combustors can give rise to local pockets of fuel-lean and fuel rich mixtures. Thereby, the burning rates and heat release rates are altered. These also lead to high concentration carbon monoxide, unburned hydrocarbons, high soot formation and exhaust smoke. Oscillations in mean droplet diameters will in turn alter the heat release. If the heat release is in phase with acoustic modes of the combustor, they may lead to combustion instability. The difference in magnitude of variation in phase averaged droplet diameters within an acoustic cycle at different locations shows that monodisperse approximation is not valid in the computational studies. The responses of droplet sizes to acoustic oscillation differ from location to location in a spray field in the presence of swirl flow. The maximum phase averaged droplet size is at phase angle of 240° in an acoustic cycle at an axial location 25 mm downstream from the atomizer exit in the presence of acoustic field (Fig. 8a). At a location 25 mm off axis, the maximum phase averaged droplet size is at a phase angle of 120° in an acoustic cycle at the axial location in the presence of acoustic field (Fig. 8b).

3.4 EFFECT OF ACOUSTIC FIELD ON DROPLET VELOCITIES

Droplet velocities in the water spray field in the swirl flow are affected by the presence of acoustic velocity oscillations. The trend in the variation of phase averaged velocities of droplets is different at on-axis and off-axis locations.

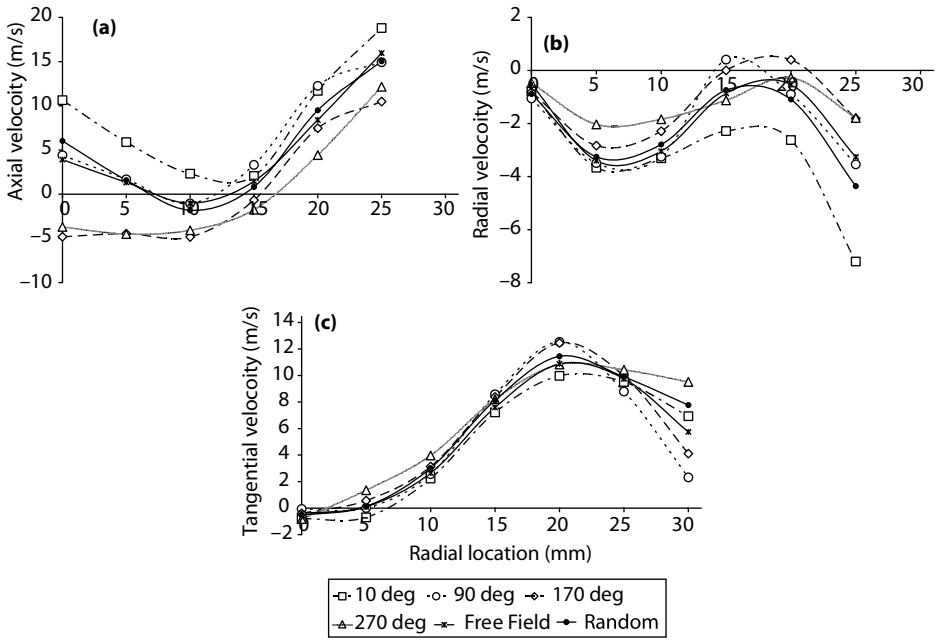

Fig. 10 Radial variation of phase averaged velocities of droplets a) axial, b) radial and c) tangential, at 25 mm downstream from the atomizer exit for 238 Hz and pressure amplitude of 3000 Pa.

Figure 10 shows the radial variation of phase averaged axial, radial and tangential velocities of the droplets within an acoustic cycle at 25 mm downstream from the atomizer exit for 238 Hz and pressure amplitude of 3000 Pa. It is observed from Fig. 10a, that the magnitude of variation in phase averaged axial velocity inside the recirculation region (i.e., within 15 mm off axis) is high compared with the locations outside the CTRZ. Variation in phase averaged axial velocity of the droplets is 16.6 m/s at axis compared to 6.2 m/s at 15 mm off axis location. Radial variation of phase averaged radial velocity plot (Fig. 10b) shows that the variation in radial velocity of the spray droplets increases within an acoustic cycle along the off axis locations. At the axis of the flow field, the axial velocity component is dominant. The swirl flow expands and disperses gradually downstream. This has a radial component associated with it. The acoustic velocity oscillations generated in the acoustic chamber is axial. This causes the swirler flow field to contract and spread out in co-flowing and counter-flowing acoustic velocities, respectively. This in turn affects the spray droplets entrained in the swirl flow field. Variation in phase averaged tangential velocity is minimal within an acoustic cycle in all radial locations (Fig. 10c) compared to that of the axial and radial phase averaged velocities. The magnitude of radial variation of random measurements of axial, radial and tangential droplet velocities in the presence of acoustic field is in the same order of mean axial, radial and tangential droplet velocities in absence of acoustic field.

The flow field is highly three dimensional in the presence of the swirl. The droplets in the spray are entrained by the three dimensional velocity fields. The CTRZ of the swirl flow field affects the mean droplet velocities of the water spray significantly compared with the droplet velocities of the spray in the absence of the swirl flow. Therefore, it is not apt to compare the droplet size and velocity measurements of the spray field in the absence and with the presence of swirl flow. However, the spray is injected into the recirculation region in the presence of swirl flow in the investigation of spray – swirl – acoustic interactions. The relative velocity between the droplets in the spray and the surrounding medium are increased in the presence of swirl flow compared to that in the absence of swirl flow. This causes the droplets to exhaust its momentum faster. Then the droplet motion is dictated by the aerodynamics of the surrounding continuous phase.

3.5 DROPLET CLUSTERING AND SIZE DISTRIBUTION

Periodic clustering of droplets in the presence of acoustic field is observed in the spray field. The investigations of water sprays in the swirl flow field are performed in ambient conditions in the presence and absence of acoustic oscillations. Figure 11a shows the bar chart of the ratio of the particle count in each 20° phase angle bin to the total particle count at 25 mm downstream along the axis from the atomizer exit. The valid droplet size measurements acquired at the investigation location are tagged with the phase angle information during acquisition. An acoustic cycle of 360° is divided into 18 bins with each bin corresponding to 20° phase angle. The acquired data is segregated into their respective phase angle bins based on the acquired phase of the valid droplet size measurement in an acoustic cycle. In the presence of acoustic field, the particle count in each bin varies in an acoustic cycle. The variation increases with increase in the acoustic pressure amplitude. The maximum particle count is 14 times the minimum count in a phase angle bin at axis in CTRZ of swirl flow for an acoustic pressure amplitude of 3000 Pa and frequency of 238 Hz (Fig. 11a). High variation of particle counts in phase angle bins at axial location within an acoustic cycle is due to high level of fluctuations in the recirculation zone [23].

Figure 11b shows the bar chart of the ratio of the particle count in each 20° phase angle bin to the total particle count of droplets in the spray field for a *We* of 33.1 at 25 mm downstream from the atomizer exit and at 25 mm off-axis. The variation increases with increase in the acoustic pressure amplitude. The maximum particle count is 3 times the minimum count in a phase angle bin at 25 mm off-axis for an acoustic pressure amplitude of 3000 Pa and frequency of 238 Hz. This location is outside the CTRZ of the swirl flow. Variations in the particle count in phase angle bins in an acoustic cycle differ in different radial locations as observed from bar charts (Fig. 11) for the same acoustic pressure amplitude and frequency of 3000 Pa and 238 Hz, respectively. Variations in the particle count in phase angle bins in an acoustic cycle is high in the recirculation region compared to the off-axis locations. This trend can be correlated with the variation in phase averaged axial velocity of the droplets in the presence of acoustic oscillations (Fig. 10a). Phase averaged axial velocity variation in an acoustic cycle is high in the recirculation region. Variation of

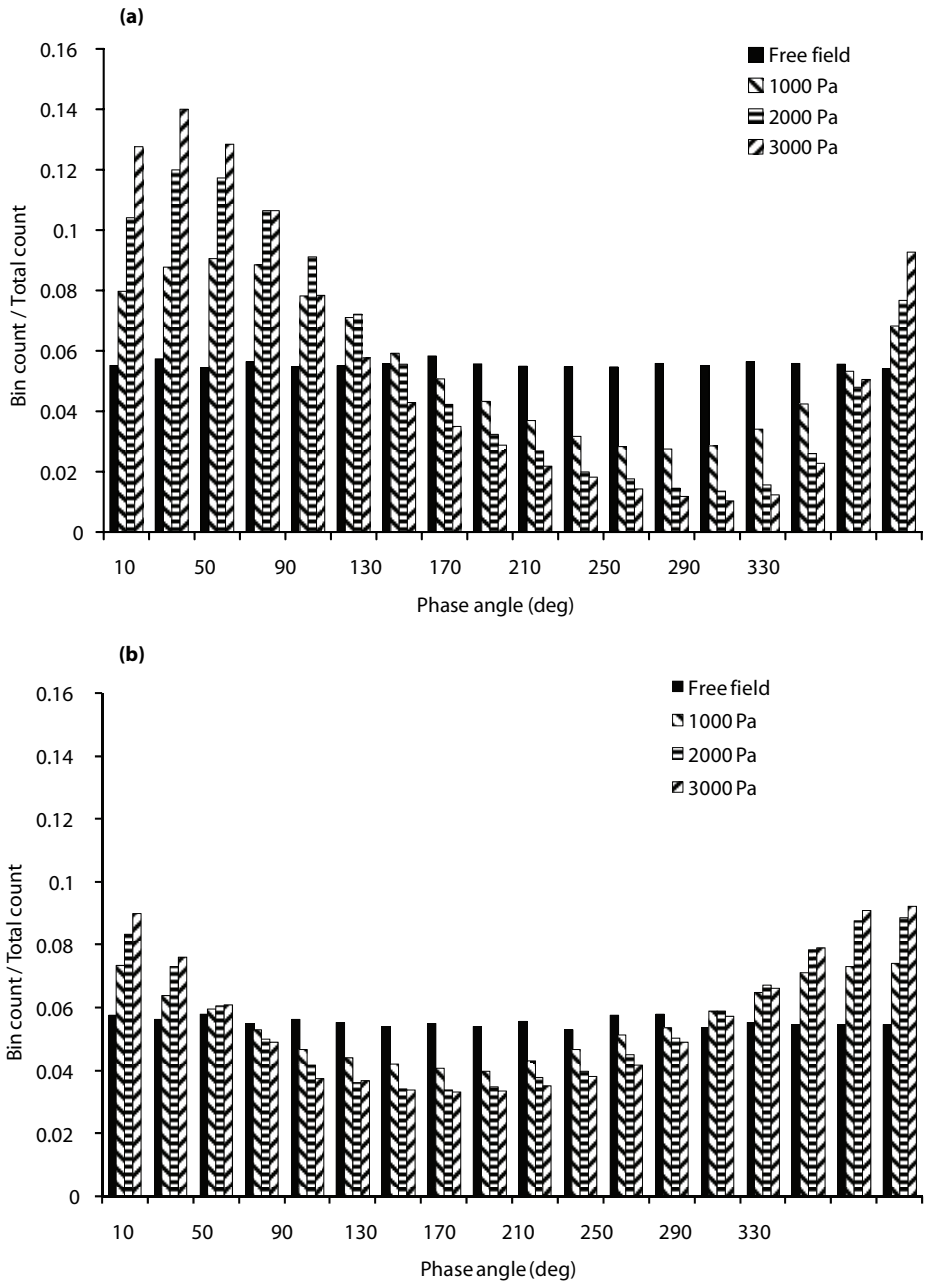

Fig. 11 Phase angle binned particle counts at different acoustic pressure amplitudes for frequency of 238 Hz at 25 mm downstream from the atomizer exit a) axis and b) 25 mm off-axis.

the particle count in an acoustic cycle could be due to the oscillations of the droplets in response to the velocity oscillations. The minimum particle count occurs in 261° to 280° phase angle bin at the axis of atomizer. However, this occurs in phase angle bins of 141° to 160° at 25 mm off-axis location of the atomizer in an acoustic cycle. The mean axial velocities of droplets in swirl flow field are 4 m/s and 16 m/s at axis and 25 mm off-axis location, respectively in the absence of acoustic field. The droplets in the off-axis locations are carried away by the swirling flow field from the centre. The spray is injected into CTRZ of swirl flow. The mean axial velocity of droplets in swirl flow field is -1 m/s at 10 mm off-axis location. This variation in the droplet velocities from location to location causes the trend in the variation in particle count to vary from location to location in the presence of acoustic field. This brings out the complexities involved in dealing with the spray – swirl interaction in the presence of acoustic field.

The variation in the droplet number density in an acoustic cycle is very high at axial locations due to presence of recirculation zone in the water spray – swirl – acoustics interactions compared to that of water spray in an acoustic field in the absence of swirl flow [11]. However, the variation of droplet count in the phase angle bins in an acoustic cycle is of the same order at the off-axis locations for both the water spray in acoustic excitation in the presence and absence of the swirl flow.

The presence of an acoustic field affects the droplet diameter distribution in the spray field in an acoustic cycle. The phase resolved diameter distribution of droplets in the spray field in an acoustic pressure amplitude of 3000 Pa and frequency of 238 Hz at 25 mm downstream along the axis from the atomizer exit is shown in Fig. 12a. The diameter distributions of the droplets in spray field are steeper at the phase angle bins between 0° to 60° in an acoustic cycle and more like a small bump in the phase angle bins between 221° to 280°. These phase angle bins coincide with maximum and minimum phase averaged axial velocity of the spray field in the presence of acoustic field, respectively with a phase lag around 30° at the axial location. Figure 12b shows the phase resolved diameter distribution of droplets in the spray field exposed to an acoustic field with a maximum pressure amplitude of 3000 Pa and frequency of 238 Hz at 25 mm downstream from the atomizer exit and at 25 mm off-axis location. The diameter distributions of the droplets in the spray field are steeper between the phase angle bins 301° to 360° in an acoustic cycle. Variation in the diameter distribution of the droplets in the presence of the acoustic field at 25 mm off-axis location does not correlate well with the phase averaged axial velocity. This may be due to the presence of sufficient radial and tangential velocity at the off-axis locations. The variation is high for small diameter bins and higher diameter bins are not affected by the velocity oscillations. The smaller diameter droplets are entrained by the acoustic velocity oscillations.

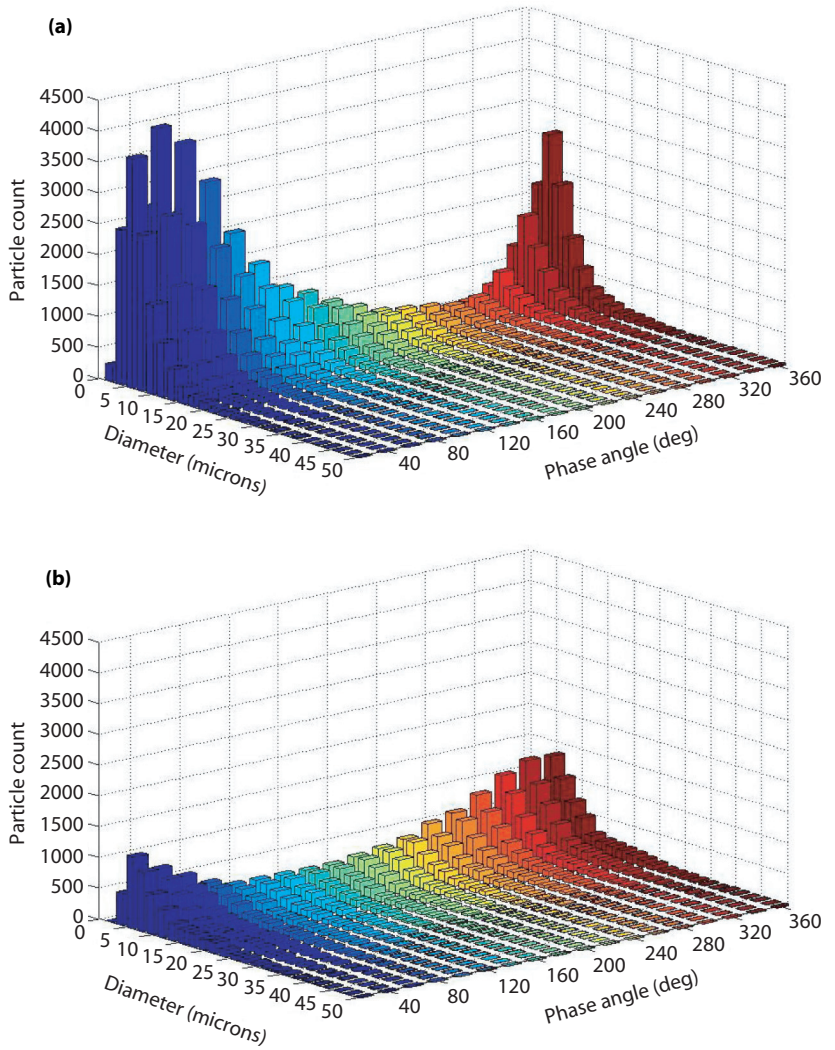

Fig. 12 Phase resolved diameter distribution of droplets in the spray field in an acoustic pressure amplitude of 3000 Pa. For frequency of 238 Hz at 25 mm downstream from the atomizer exit a) axis and b) 25 mm off-axis.

4. CONCLUSION

An experimental investigation of water spray – swirl – acoustic interactions was performed using planar Mie scattering, phase Doppler particle size analyzer and laser Doppler velocimetry. Planar spray visualization in the presence and absence of swirl flow revealed that the spray is altered drastically in the presence of strong swirl flow. The phase averaged droplet diameter of the spray in swirl flow varies in an acoustic cycle. A variation of 50% in D_{10} phase averaged diameter within an acoustic cycle over the mean

diameter is observed for an acoustic pressure amplitude of 3000 Pa. The magnitude of variation in the phase averaged droplet diameter, D_{10} within an acoustic cycle varies from location to location. In the presence of acoustic excitation, the magnitude of variation of phase averaged axial velocity of droplets is high compared to the variation of phase averaged radial and tangential velocities of the droplets in the water spray in swirl flow. The variation in the recirculation velocity of the swirl flow is high in the CTRZ in the presence of an acoustic field. This in turn alters the velocity of the spray and the surrounding medium, affecting the droplet size and the axial velocity variation in an acoustic cycle. The axial velocity oscillation of the droplets in the recirculation zone is as high as 200% compared with that of acoustic velocity oscillations. High variation of particle counts in phase angle bins at axial location within an acoustic cycle (14 times the minimum) is due to high level of fluctuations in the recirculation zone in the presence of acoustic oscillations. The droplet size distribution varies within an acoustic cycle in the presence of acoustic oscillations and with radial location.

ACKNOWLEDGEMENTS

The authors wish to acknowledge the financial support of Aeronautical Research and Development Board of India. The authors wish to thank S. R. Chakaravarthy for useful discussions on this work.

REFERENCES

[1] A. H. Lefebvre, Fifty Years of Gas Turbine Fuel Injection, *Atomization and Sprays,* 2000, 10, 251-276.

[2] A. H. Lefebvre, Gas Turbine Combustion, *Taylor & Francis*, USA.

[3] A. K. Gupta, D. G. Lilley and N. Syred, Swirl Flows, *Abacus Press*, Tunbridge Wells, Kent.

[4] A. Rizkalla, and A. H. Lefebrve, The Influence of Air and Liquid Properties on Airblast Atomization, *ASME J. Eng. Gas Turbine Power*, 1975, 97(3), 316-320.

[5] C. Presser, A. K. Gupta and H. G. Semerjian, Aerodynamic characteristics of swirling spray flames: pressure-jet atomizer, *Combustion and Flame*, 1993, 91(1-2), 31-44.

[6] C. Presser, A. K. Gupta, H. G. Semerjian and C. T. Avedisian, Droplet transport in a swirl-stabilized spray flame, *Journal of Propulsion and Power,* 1994, 10(5), 631

[7] C. Presser, A. K. Gupta, J. T. Hodges and C. T. Avedisian, Interpretation of size-classified droplet velocity data in swirling spray flames, *AIAA – 1995 – 283, 33rd AIAA Aerospace Sciences Meeting and Exhibit,* 9-12 January, Reno, Navada.

[8] A. K. Gupta, C. Presser, J. T. Hodges and C. T. Avedisian, Role of combustion on droplet transport in pressure-atomized spray flames, *Journal of Propulsion and Power,* 1996, 12(3), 543

[9] S. M. Jeng, N. M. Flohre and H. C. Mongia, Fluid property effects on non-reacting spray characteristics issued from a counter-rotating swirler, *AIAA – 2005 – 356, 43rd AIAA Aerospace Sciences Meeting and Exhibit,* 10 – 13 January, Reno, Navada.

[10] M. C. McQuay, and R. K. Dubey, The interaction of well-characterized longitudinal acoustic waves with a nonreacting spray, *Atomization and Sprays*, 1998, 8, 419-437.

[11] R. K. Dubey, D. L. Black, M. Q. McQuay and J. A. Carvalho, Jr (1997) The effect of acoustics on an ethanol spray flame in a propane-fired pulse combustor, *Combustion and Flame,* 110, 25-38.

[12] R. I. Sujith, An experimental investigation of interaction of sprays with acoustic fields, *Experiments in Fluids*, 2005, 38, 566-587.

[13] R. Kumara Gurubaran and R. I. Sujith, An Experimental Investigation of Non-Evaporative Sprays in Axial Acoustic Fields, *AIAA-2008-1046, 46th AIAA Aerospace Sciences Meeting and Exhibit*, 7-10 January 2008, Grand Sierra Resort Reno, Nevada.

[14] J. R. Dawson, V. M. Rodriguez-Martinez, N. Syred and T. O'Doherty, The effect of combustion instability on the structure of recirculation zones in confined swirling flames, *Combustion Science and Technology*, 2005, 177, 2349-2371.

[15] T. J. Anderson, D. W. Kendrick, J. M. Cohen and T. J. Rosfjord, Measurement of spray/acoustic coupling in gas turbine fuel injectors, *Symposium on Gas Turbine Engine Combustion, Emissions and Alternative Fuels,* 12-19 October 1998, Lisbon, Portugal.

[16] A. Brena de la Rosa, G. Wang and W. D. Bachal, The Effect of Swirl on the Velocity and Turbulence Fields of a Liquid Spray, *Transactions of the ASME*, 1992, 114, 72-81.

[17] P. Gajan, B. Strzelecki, B. Platet and R. Lecourt, Investigation of spray behavior downstream of an aeroengine injector with acoustic excitation, *Journal of Propulsion and Power*, 2007, 23(2), 390-397.

[18] E. Arunraj, R. I. Sujith and S. R. Chakravarthy, Investigation of effect of acoustic oscillations on swirl flow using PIV, *AIAA-2009-3700, 39th AIAA Fluid Dynamics Conference*, 22-25 June 2009, San Antonio, Texas.

[19] R. Payri, L. Araneo, J. Shakal and V. Soare, Phase Doppler measurements: System set-up optimization for characterization of a diesel nozzle, *Journal of Mechanical Science and Technology*, 2008, 22, 1620-1632.

[20] Y. Hardalupas, A. M. K. P. Taylor and J. H. Whitelaw, Velocity and size characteristics of liquid-fuelled flames stabilized by a swirl burner, Proceedings of Royal Society of London, 1990, A 428, 129-155.

[21] V. A. Iyer and M. A. Woodmansee, "Uncertainty Analysis of Laser-Doppler-Velocimetry Measurements in a Swirling Flowfield", AIAA Journal, Vol. 43 (3), 2005, pp. 512-519.

[22] G. E. Lorenzetto and A. H. Lefebvre, Measurements of Drop Size on a Plain-Jet Airblast Atomizer, *AIAA Journal,* 1977, 15, 1006-1010.

[23] R. Kumara Gurubaran and R. I. Sujith, An Experimental Investigation of Swirl Flow in Axial Acoustic Fileds, *AIAA-2009-785, 47th AIAA Aerospace Sciences Meeting and Exhibit*, 5-8 January 2009, Orlando, Florida.

[24] R. Kumara Gurubaran, Behavior of Sprays in Acoustic Fields, *Ph. D. Thesis*, Indian Institute of Technology Madras, 2009.